Reaction mechanism of ^{8}B breakup at the Fermi energy

S. L. Jin (金仕纶),[1,2] J. S. Wang (王建松),[1,*] Y. Y. Yang (杨彦云),[1] P. Ma (马朋),[1] M. R. Huang (黄美容),[1] J. B. Ma (马军兵),[1] F. Fu (付芬),[1] Q. Wang (王琦),[1] M. Wang (王猛),[1] Z. Y. Sun (孙志宇),[1] Z. G. Hu (胡正国),[1] R. F. Chen (陈若富),[1] X. Y. Zhang (张雪荧),[1] X. H. Yuan (袁小华),[1] X. L. Tu (涂小林),[1] Z. G. Xu (徐志国),[1] K. Yue (岳珂),[1] J. D. Chen (陈金达),[1] B. Tang (唐彬),[1] Y. D. Zang (臧永东),[1] D. P. Wu (武大鹏),[1] Q. Hu (胡强),[1] Z. Bai (白真),[1] Y. J. Zhou (周远杰),[1,2] W. H. Ma (马维虎),[1,2] J. Chen (陈杰),[1,2] C. J. Lin (林承键),[3] X. X. Xu (徐新星),[3] Z. Z. Ren (任中洲),[4] C. Xu (许昌),[4] D. D. Ni (倪冬冬),[4] Y. H. Zhang (张玉虎),[1] H. S. Xu (徐瑚珊),[1] and G. Q. Xiao (肖国青)[1]

[1]*Institute of Modern Physics, Chinese Academy of Sciences, Lanzhou 730000, China*

[2]*University of Chinese Academy of Sciences, Beijing 100049, China*

[3]*Institute of Nuclear Physics, China Institute of Atomic Energy, Beijing 102413, China*

[4]*Department of Physics, Nanjing University, Nanjing 210008, China*

(Received 16 February 2015; revised manuscript received 28 April 2015; published 28 May 2015)

The longitudinal momentum distributions of ^{7}Be fragments in the breakup of ^{8}B on a carbon target have been measured at 36 MeV/u. The different mechanisms have been distinguished by coincidence measurements. The longitudinal momentum distributions of ^{7}Be fragments from both the stripping and the diffraction mechanisms are consistent with the results of noneikonal calculations and CDCC calculations. The full widths at half maximum of the longitudinal momentum distributions are 124 ± 17 and 92 ± 7 MeV/c for the stripping and diffraction components, respectively. The comparison with the different model calculations is discussed. It is crucial to separate the different reaction mechanisms experimentally to benchmark nuclear reaction theories.

DOI: 10.1103/PhysRevC.91.054617 PACS number(s): 21.10.Gv, 24.50.+g

I. INTRODUCTION

Exotic structure is one of the hot topics in nuclear physics accessible with radioactive beams. Neutron halos, consisting of extended neutron distributions coupled to a core, have been found for many weakly bound neutron-rich nuclei such as ^{11}Li and ^{11}Be [1–3]. The proton drip-line nucleus ^{8}B, with a proton separation energy of 136.4 keV [4], has attracted intense experimental and theoretical attention because it is the most likely a nucleus with a proton halo. However, it is rather controversial whether the halo structure of ^{8}B exists. Many different pieces of evidence argue for a proton halo. The interaction cross section at relativistic energy indicates that the root-mean-square (rms) radius of ^{8}B is different from more tightly bound Boron isotopes [1,5]. The systematic study of nuclear matter radii shows that ^{8}B has a large proton matter radius compared to its neutron matter radius [6]. The enhanced reaction cross section extracted by angular distribution measurements at sub-Coulomb [7] and intermediate energies [8–10] and the large proton-removal cross section at relativistic and intermediate energies with different targets [8,11,12] support the case for a halo structure of ^{8}B. The rms radius obtained from asymptotic normalization coefficient (ANC) for the last proton in ^{8}B is much larger than the rms radius of the ^{7}Be core [13]. There are also a few experimental results that argue against the proton halo structure of ^{8}B. The measured total reaction cross sections at relativistic energy are not obviously enhanced in Refs. [14,15]. The one-proton removal cross section does not support a substantial halo of ^{8}B [16]. The large quadruple moment of ^{8}B can also be explained by the polarization of the ^{7}Be core instead of a halo structure [17,18].

As the narrow longitudinal momentum distribution of the ^{7}Be fragment from breakup reactions is regarded as prominent evidence of an extended structure of ^{8}B, many measurements of the ^{7}Be longitudinal momentum distributions have been performed. The experiment at GSI with 1471 MeV/u beam energy showed a narrow full width at half maximum (FWHM) width of 81 ± 6 MeV/c [19], and then the FWHM values were measured as 91 ± 5 and 95 ± 5 MeV/c at the beam energies of 1440 MeV/u [12] and 936 MeV/u [14], respectively. At Grand Accelerateur National d'Ions Lourds the FWHM value was determined to be 93 ± 7 MeV/c at ^{8}B beam energy of 38 MeV/u [8]. In Ref. [20], longitudinal momentum distribution measurements were performed at Michigan State University (MSU) at the beam energy of 41 MeV/u and the FWHM are 81 ± 4 and 62 ± 3 MeV/c on a Be target and a Au target, respectively. Calculations with the valence proton in the $p_{3/2}$ state in Woods-Saxon potential give 160 MeV/c for the ^{7}Be fragment longitudinal momentum distribution on a Be target, which is much wider than the experimental data. With more detailed treatment of the proton stripping process, the FWHM is reduced to 82 MeV/c and in agreement with the experimental data [21]. The diffraction breakup reaction was not treated because it is more difficult, but it is estimated to have a similar width [22]. The stripping and diffraction mechanisms involved in breakup reactions were clearly identified for the first time in Ref. [23] and both stripping and diffraction components of the one-proton knockout cross sections for ^{8}B were measured at 86.7 MeV/u.

In this paper new experimental data for the breakup of ^{8}B on a Carbon target at 36 MeV/u are reported. By employing coincidence measurements of the residue and proton following breakup reaction, we present the longitudinal momentum distributions of ^{7}Be from both stripping and diffraction mechanisms of a ^{8}B breakup reaction at near Fermi

*jswang@impcas.ac.cn

energy. Our experimental data show that the FWHM from the diffraction mechanism is slightly narrower than that from the stripping mechanism. A brief description of the experimental setup and an outline of the data analysis are given in Sec. II. In Sec. III the measured longitudinal momentum distributions are compared with results of theoretical calculations and the results are discussed. In Sec. IV the main conclusions of this work are summarized.

II. EXPERIMENTAL SETUP AND DATA ANALYSIS

The experiment was carried out at the Radioactive Ion Beam Line in Lanzhou (RIBLL) [24,25]. The primary beam was 80.1 MeV/nucleon ^{12}C delivered by the Heavy Ion Research Facility of Lanzhou (HIRFL) [26,27]. The RIBs were produced by bombarding the Be production target with a thickness of 4171 μm. The RIB beam was analyzed and delivered to the secondary reaction chamber at the second focal point of the RIBLL. To improve the purity of the selected secondary RIBs, a 1112-μm-thick Al wedge was used as a degrader at the first focal plane of the RIBLL. To identify the radioactive beams two 50-μm plastic scintillation detectors were installed at two focal points of the RIBLL with a separation distance of 17 m and used as time-of-flight detectors. These were employed together with magnetic rigidity and energy-loss measurements (a 325-μm silicon detector). For the same magnet setting, the purity of ^{8}B is 44%; the contaminants of 40% ^{9}C, 13% ^{7}Be, and 3% ^{6}Li ions were also delivered. In the secondary reaction chamber, two position-sensitive parallel-plate avalanche counters (PPACs) [28] provided the position of the incoming beams with a position resolution better than 1 mm. Each PPAC had 50 gold-plated tungsten wires in both X and Y directions and a sensitive area of 50×50 mm^2. The distances of PPAC1 and PPAC2 from the secondary target were 760 and 280 mm, respectively. The position and incident angle of the beam particles at the target were determined by extrapolating the position information provided by PPAC1 and PPAC2 event by event.

The carbon target was a self-supported foil with a thickness of 45 mg/cm^2. A ΔE-E telescope array covering the polar angles -17° to 17° in the laboratory frame was used to measure the reaction products. A detailed description of this telescope array can be found in Ref. [29]. The first part of the telescope array is a ΔE detector, a double-sided silicon strip detector

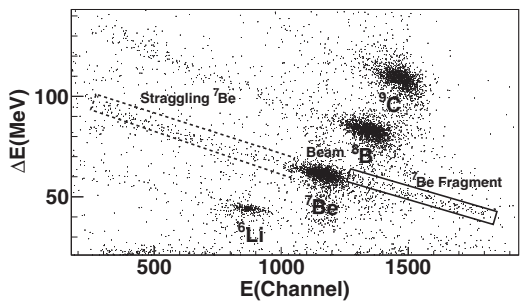

FIG. 1. Typical ΔE-E particle identification spectrum. The solid outline rectangle encloses events corresponding to breakup reaction from ^{8}B or ^{9}C; the dashed rectangle encloses events corresponding to the straggling ^{7}Be.

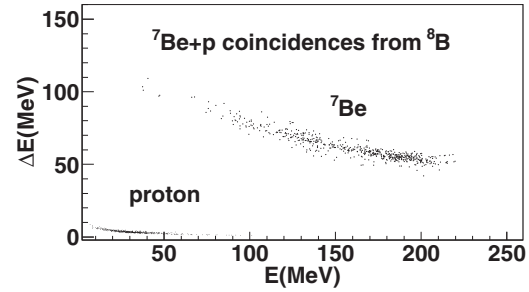

FIG. 2. The ΔE-E spectrum coincidence proton and ^{7}Be in breakup reactions from ^{8}B.

(DSSD) with a thickness of 1000 μm and a sensitive area of 40×40 mm^2, which is divided into 40 strips in each side. The second part is an E detector, a CsI(Tl) crystal array which is composed of 64 (8×8) CsI(Tl) crystals [30]. The active area of each crystal unit is 21×21 mm^2 for the front side and 23×23 mm^2 for the back side; the length of each crystal is 50 mm. Thus, the maximum energies stopped in one crystal can reach 133 MeV for protons.

A typical ΔE-E particle identification spectrum obtained in the telescope array is shown in Fig. 1. ΔE is the energy loss from the DSSD detector and E is the residual energy deposited the CsI(Tl) crystal. A clear separation of different nuclei is obtained. Three different regions on the ^{7}Be line are identified as the straggling ^{7}Be, the ^{7}Be resulting from the elastic scattering in the C target and the ^{7}Be produced from the breakup of ^{8}B or ^{9}C. With the time-of-flight signal of ^{8}B, the events from one-proton knockout reactions have been selected event by event. Figure 2 shows the ΔE-E plots for the coincidence measurement of ^{7}Be and proton breakup from ^{8}B.

In these coincidence events both elastic (diffraction) and inelastic (stripping) interactions with the target are included. To distinguish these different mechanisms, the excitation energy spectrum of ^{8}B is reconstructed event by event using the energies of the detected ^{7}Be and protons. A similar method has been performed at MSU [23,31]. As shown in Fig. 3, there are two peaks: The sharp peak at high energy corresponds to the events that there is barely energy transfer to the target

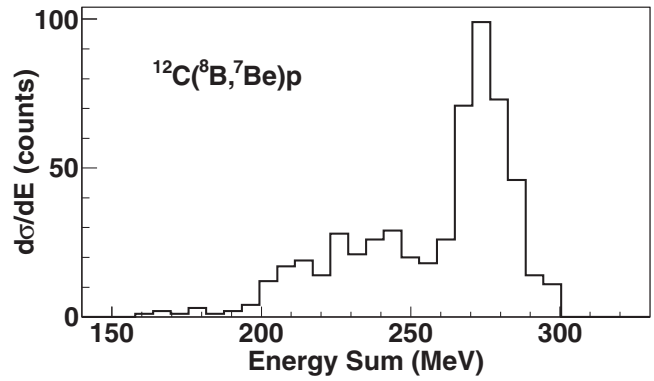

FIG. 3. Energy sum spectra of the one-proton knockout residue ^{7}Be and the proton detected in coincidence in the telescope array for ^{8}B. The sharp peak corresponds to elastic breakup (diffraction mechanism); the broad peak corresponds to inelastic breakup (stripping mechanism).

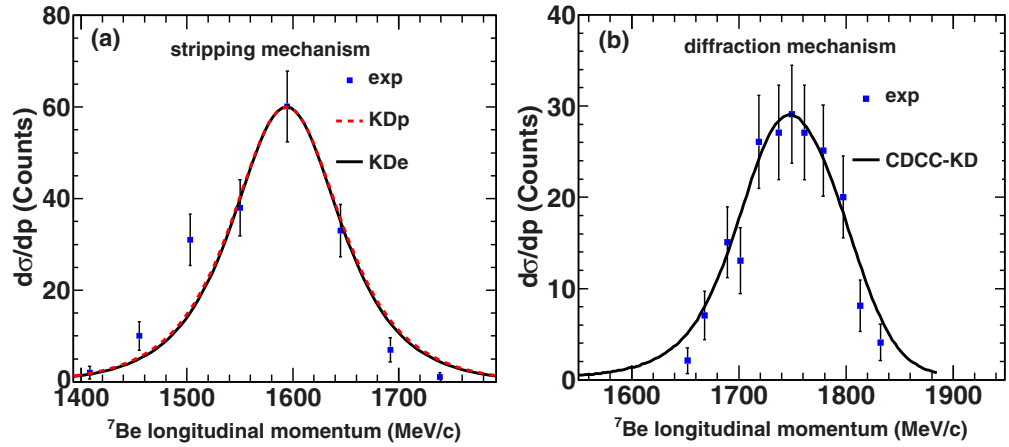

FIG. 4. (Color online) The longitudinal momentum distributions of ^{7}Be fragments from the breakup of ^{8}B on a C target. Shown for diffraction (a) and stripping (b) mechanisms. In (a) the black solid line represents results of the KDe calculation and the red dashed line presents results of the KDp calculation (see text for definitions). In (b) the red dashed line represents results from CDCC with KD potential. Both the experimental data and model calculation include the experimental broadening.

nucleus and that the total initial ^{8}B kinetic energy is shared by the fragments, ^{7}Be, and proton. Events in this peak are classified as the elastic breakup. A broad peak at lower energy shows the events identified as the inelastic breakup because a part of the initial kinetic energy of the ^{8}B is lost to excite the target nucleus. The diffractive part contributes 55% to the experimental data, and the remaining 45% comes from stripping part. When we see 38% of diffraction and 62% of stripping in higher energy experiment [23], it can be inferred that the ratio of diffraction/stripping depends on the incident energy.

With the energy measured by the ΔE-E telescope array and the position from PPACs and DSSD, the longitudinal momentum distributions of ^{7}Be from both stripping and diffraction mechanisms are obtained as shown in Fig. 4. There are some effects broadening the distribution, such as the energy spread of the incoming ^{8}B, the energy resolution of the telescope detector, and the energy spread in the carbon target. Collectively, they have a FWHM of 49 MeV/c. After corrections are made for these extraneous effects, the FWHMs of ^{7}Be longitudinal momentum distribution in the laboratory frame are 92 ± 7 and 124 ± 17 MeV/c, corresponding to the diffraction and stripping mechanisms, respectively.

III. THEORETICAL ANALYSIS

Effective three-body model calculations have been performed [32]. The complex ^{7}Be-target optical potential was calculated using the double-folding method of Ref. [33], assuming Gaussian ^{7}Be and ^{12}C densities of rms radii 2.31 and 2.32 fm [34]. The proton-target potential was calculated from the Koning and Delaroche global parametrization [35]. The stripping momentum distributions were calculated using the eikonal approximation formalism [36] and the eikonal phase shifts and S matrices of the above potentials (denoted KDe). In addition, owing to the relatively low beam energy, calculations were repeated using the improved (exact continued [37]) description of the proton-target S matrix (denoted KDp). The ^{8}B(g.s.) to ^{7}Be final-state radial overlaps and spectroscopic factors were taken from Ref. [23]. The diffraction mechanism differential cross sections were calculated using a CDCC breakup model space [23], and the resulting momentum distributions were constructed by integration over the solid angles covered by the current detection system, as discussed in Ref. [38]. All theoretical momentum distributions are folded with a FWHM (Gaussian) experimental resolution of 49 MeV/c.

It is worth noting that the present experimental data show that the distribution from stripping is broader than that for diffraction. Although the theoretical calculations of stripping are a little wider than the those of the diffractive part, both of them are quite similar.

The experimental and theoretical FWHMs for stripping and diffraction are summarized in Table I. Hansen calculated the ^{7}Be longitudinal momentum distributions with eikonal model [22], the total single-particle wave function calculated in a Woods-Saxon potential gave a FWHM of 153 MeV/c. After the localized wave function, the distributions were reduced to 75 MeV/c and in agreement with the GSI experimental data [19] at high energies. In Ref. [21], the Serber model with transparent limit predicted the total ^{7}Be longitudinal momentum distributions of 166 MeV/c. Neglecting $m_l = 0$ contributions, the FWHM is 104 MeV/c. Considering the strong absorption in the target (opaque limit) the distributions were reduced to 82 MeV/c. In Ref. [39], both stripping and diffraction are considered in the models developed by Serber [40] and Glauber [41] to describe the breakup reactions; the interactions in this model are taken from a realistic optical potential at low energies and from total nucleon-nucleon cross sections at high energy. With this model, FWHMs of 93 MeV/c for the diffraction mechanism and 151 MeV/c for the stripping mechanism with transparent limit were obtained. This result shows an obvious difference between the two mechanisms; because the interactions in this model are suitable for high energy near GeV/u at the Fermi energy of the present work, it may not describe the experiment approximately. The present calculation, however, with more accurate details in the model, shows that the distributions of the two mechanisms are

TABLE I. Summary of the distributions measured in this work and calculated in different model.

	Present work (MeV/c)	KD (MeV/c)	KDe (MeV/c)	KDp (MeV/c)	Hencken (MeV/c)	Hensen (MeV/c)	Esbensen (MeV/c)
Stripping	124(17)		103	107	151	153/75	166/82
Diffraction	92(7)	101			93		

similar, which is closer to the experimental data than previous calculation [39]. In Ref. [21,22], although the diffraction distribution is not presented, the author indicated that it would be similar with the stripping distribution; it shows the same tendency with the present calculation.

^{8}B is really an interesting nucleus at the proton drip line. The elastic scattering studies of ^{8}B have shown its strange behavior relative to that of the neutron halo nuclei [42]. Theoretical calculations [43] indicated that the longitudinal momentum distributions of core fragments from proton stripping reactions could provide experimental insight into the structure of the halo states and the role played by the reaction mechanism. Subsequent experiments substantiated this [44]. In the present experiment, the distribution for the diffractive mechanism is quite similar to previous data that argue for the halo structure of ^{8}B. For the wider distribution seen in stripping we may infer that reaction mechanisms influence the connection between halo size and momentum distributions.

IV. SUMMARY

In summary, the longitudinal momentum distributions of ^{7}Be have been measured for the breakup of ^{8}B at 36 MeV/u on a carbon target. For the first time longitudinal momentum distributions for both the stripping and diffraction mechanisms have been obtained by a coincidence technique. In a comparison with results of previous theoretical calculations with the Serber model, our results lead to the conclusion that the distributions in the diffraction part are in good agreement. The present experimental data show a marginal difference of the longitudinal momentum distributions between stripping and diffraction. Theoretical calculations show the same tendency. It is important to separate the reaction mechanisms experimentally to benchmark reaction theories.

ACKNOWLEDGMENTS

We would like to acknowledge the staff of HIRFL for the operation of the cyclotron and friendly collaboration. We are grateful to George Bertsch, Carlos Bertulani, and Henning Esbensen for informative discussions. This work was financially supported by the National Basic Research Program of China (973 Programs No. 2014CB845405 and No. 2013CB834403) and the National Natural Science Foundation of China (Grants No. U1432247, No. 11075190, No. 11205209, and No. 11205221).

[1] I. Tanihata *et al.*, Phys. Rev. Lett. **55**, 2676 (1985).
[2] I. Tanihata *et al.*, Phys. Lett. B **206**, 592 (1988).
[3] P. G. Hansen and B. Jonson, Europhys. Lett. **4**, 409 (1987).
[4] M. Wang *et al.*, Chin. Phys. C **36**, 1603 (2012).
[5] M. M. Obuti *et al.*, Nucl. Phys. A **609**, 74 (1996).
[6] J. S. Wang *et al.*, Nucl. Phys. A **691**, 618 (2001).
[7] V. Guimaraes *et al.*, Phys. Rev. Lett. **84**, 1862 (2000).
[8] F. Negoita *et al.*, Phys. Rev. C **54**, 1787 (1996).
[9] M. Fukuda *et al.*, Nucl. Phys. A **656**, 209 (1999).
[10] R. E. Warner *et al.*, Phys. Rev. C **52**, R1166 (1995).
[11] B. Blank *et al.*, Nucl. Phys. A **624**, 242 (1997).
[12] M. H. Smedberg *et al.*, Phys. Lett. B **452**, 1 (1999).
[13] F. Carstoiu, L. Trache, C. A. Gagliardi, R. E. Tribble, and A. M. Mukhamedzhanov, Phys. Rev. C **63**, 054310 (2001).
[14] D. Cortina-Gil *et al.*, Phys. Lett. B **529**, 36 (2002).
[15] D. Cortina-Gil *et al.*, Nucl. Phys. A **720**, 3 (2003).
[16] I. Pecina *et al.*, Phys. Rev. C **52**, 191 (1995).
[17] T. Minamisono *et al.*, Phys. Rev. Lett. **69**, 2058 (1992).
[18] A. Csoto, Phys. Lett. B **315**, 24 (1993).
[19] W. Schwab *et al.*, Z. Phys. A **350**, 283 (1995).
[20] J. H. Kelley *et al.*, Phys. Rev. Lett. **77**, 5020 (1996).
[21] H. Esbensen, Phys. Rev. C **53**, 2007 (1996).
[22] P. G. Hansen, Phys. Rev. Lett. **77**, 1016 (1996).
[23] D. Bazin *et al.*, Phys. Rev. Lett. **102**, 232501 (2009).
[24] Z. Sun *et al.*, Chin. Phys. Lett. **15**, 790 (1998).
[25] Z. Sun *et al.*, Nucl. Instrum. Methods Phys. Res., Sect. A **503**, 496 (2003).
[26] J. W. Xia *et al.*, Nucl. Instrum. Methods Phys. Res., Sect. A **488**, 11 (2002).
[27] W. L. Zhan *et al.*, Nucl. Phys. A **805**, 533c (2008).
[28] P. Ma *et al.*, At. Energy Sci. Technol. **45**(3), 356 (2011).
[29] S. L. Jin *et al.*, Nucl. Instrum. Methods Phys. Res., Sect. B **317**, 728 (2013).
[30] X. W. Yao *et al.*, At. Energy Sci. Technol. **44**(3), 358 (2011).
[31] K. Wimmer *et al.*, Phys. Rev. C **90**, 064615 (2014).
[32] J. A. Tostevin (private communication).
[33] J. A. Tostevin and B. A. Brown, Phys. Rev. C **74**, 064604 (2006).
[34] A. Ozawa *et al.*, Nucl. Phys. A **691**, 599 (2001).
[35] A. J. Koning and J. P. Delaroche, Nucl. Phys. A **713**, 231 (2003).
[36] C. A. Bertulani and P. G. Hansen, Phys. Rev. C **70**, 034609 (2004).
[37] J. M. Brooke, J. S. Al-Khalili, and J. A. Tostevin, Phys. Rev. C **59**, 1560 (1999).
[38] J. A. Tostevin *et al.*, Phys. Rev. C **66**, 024607 (2002).
[39] K. Hencken, G. Bertsch, and H. Esbensen, Phys. Rev. C **54**, 3043 (1996).
[40] R. Serber, Phys. Rev. **72**, 1008 (1947).
[41] R. J. Glauber, Phys. Rev. **99**, 1515 (1955).
[42] Y. Y. Yang *et al.*, Phys. Rev. C **87**, 044613 (2013).
[43] B. A. Brown and P. G. Hansen, Phys. Lett. B **381**, 391 (1996).
[44] A. Navin *et al.*, Phys. Rev. Lett. **81**, 5089 (1998).